ACS APPLIED MATERIALS & INTERFACES

Research Article

www.acsami.org

Optically Active Microspheres Constructed by Helical Substituted Polyacetylene and Used for Adsorption of Organic Compounds in Aqueous Systems

Junya Liang, Ci Song, and Jianping Deng*

State Key Laboratory of Chemical Resource Engineering and College of Materials Science and Engineering, Beijing University of Chemical Technology, Beijing 100029, China

Supporting Information

ABSTRACT: This article reports optically active microspheres consisting of chiral helical substituted polyacetylene and β-cyclodextrin-derivative (β-CD-A). The microspheres showed remarkable adsorption toward various organic compounds in water. To prepare the microspheres, an acetylenic-derived helical macro-monomer was synthesized and then underwent aqueous suspension copolymerization with octadecyl acrylate and butyl acrylate by using azobis(isobutyronitrile) as initiator and β-CD-A simultaneously as comonomer and cross-linking agent. The helical macromonomer chains enabled the microspheres to exhibit desirable enantio-differentiating adsorption capacity toward chiral compounds respectively dissolved in organic solvent, dispersed in water, and dissolved in water. The saturated absorbency toward (*R*)-(+)- and (*S*)-(−)-1-phenylethylamine was 29 and 12 mg·g^{-1}, respectively. The microspheres also showed large oil absorbency (e.g., 22 g·g^{-1} CCl_4) and a large adsorption toward methyl red (as a model for organic dyes) dispersed in water. The presence of β-CD-A moieties improved the adsorption performance of the microspheres. The present optically active microspheres open a new approach for preparing adsorbents particularly chiral adsorbents with potentials for wastewater treatment.

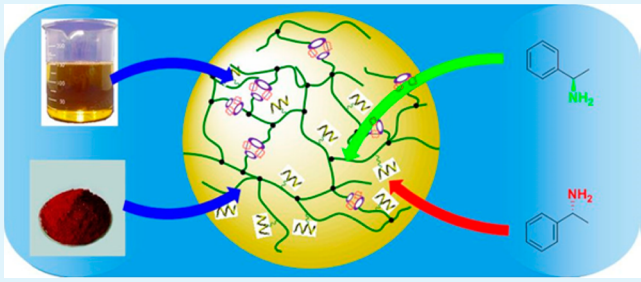

KEYWORDS: *adsorbent, chiral compound, helical polymer, microsphere*

1. INTRODUCTION

Wastewater treatment is a vital issue due to industrial wastewater discharge, overuse of pesticides, leakage of chemical materials, among other reasons.[1,2] Ever-increasing attention has been attracted to developing cleanup materials for wastewater treatment. So far, a variety of elegant adsorbents have been created to remove the pollutants, ranging from inorganic[3] and carbon[4] materials to natural[5,6] and synthetic polymer[7] materials. Cyclodextrins formed a unique category of adsorbents due to the distinctive structures.[8] More recently, some new materials were fabricated and investigated as adsorbents, such as magnetic materials,[9] metal−organic frameworks,[10] molecularly imprinted polymers,[11] and nanoscaled materials.[12] The extensively investigated adsorbates include metal ions,[13,14] organic dyes,[15] and pharmaceuticals.[16,17] However, studies dealing with chiral contaminants for instance chiral drugs and chiral pesticides, are still relatively limited. Meanwhile, novel adsorbents with the ability to simultaneously adsorb multiple types of adsorbates are also highly required.

Reportedly, over 50% of the clinical drugs and up to 25% of the pesticides are of chirality, and currently, these ratios are still continuously increasing. Chiral drugs derived from individual enantiomers frequently demonstrate varied distribution, metabolism, excretion, toxicity, and biodegradation properties.[18] Additionally, drugs in the form of racemate instead of enantiospecific forms were used over a long period, and some of them are still in use at present. All the above practical facts lead to an essential issue, namely, enantiopure compounds gradually accumulate in the environment, which may result in vital effects to organisms, since enantiomers stereoselectively react in biological systems, for instance, with enzymes. Accordingly, removal of the residual chiral compounds from environment becomes a key issue. In fact, this issue has evoked growing attention nowadays.[19−22]

Recent years have witnessed the development of chiral polymers and novel materials thereof, such as chiral (hydro)gels,[23,24] chiral nano- and microspheres,[25,26] chiral assemblies,[27,28] chiral sensor materials,[29] etc. The chiral materials held promises in chiral recognition/adsorption,[30,31] asymmetric catalysis,[32] chiral resolution,[33] enantioselective crystallization,[34,35] etc. Based on the academic background aforementioned and our earlier investigations dealing with chirally helical polyacetylenes,[35−37] we in the present study attempt to prepare a unique class of chiral microspheres composed of optically

Received: July 26, 2014
Accepted: October 7, 2014
Published: October 7, 2014

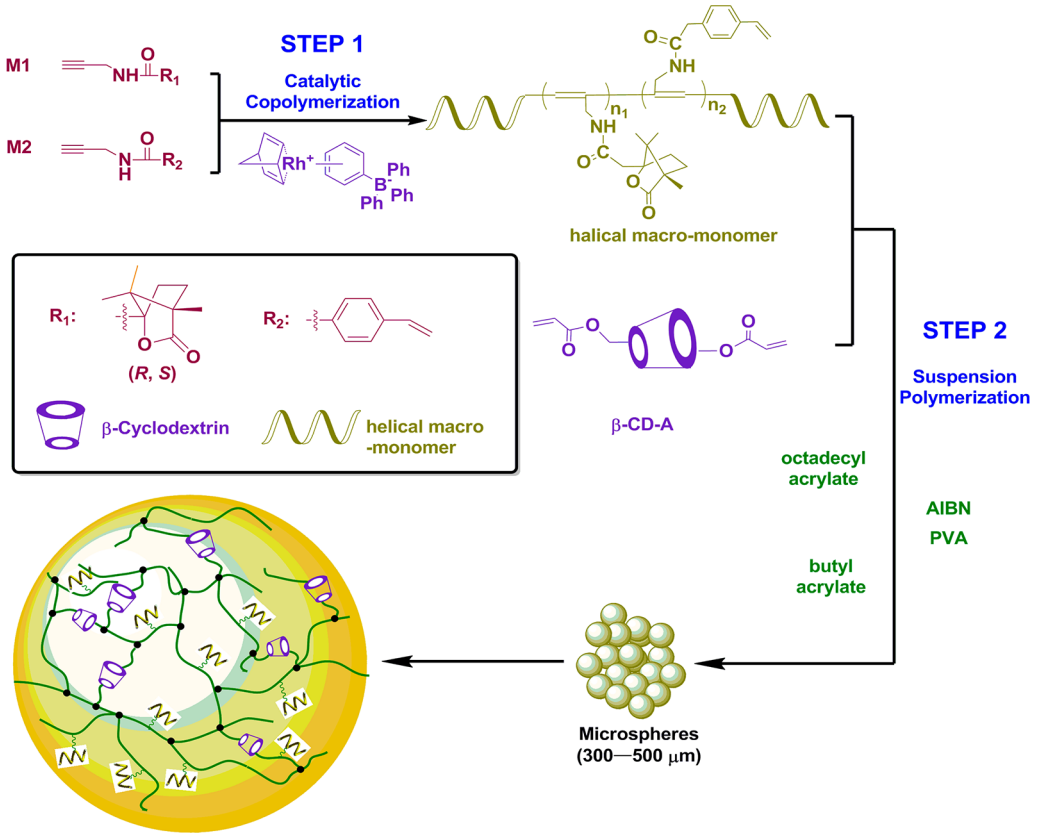

Figure 1. Schematic representation for preparing cross-linked microspheres containing helical macro-monomer and *β*-CD-A.

active helical polyacetylene and *β*-cyclodextrin derivative (*β*-CD-A). The helical polyacetylene is expected to provide chirality for the resulting microspheres, while *β*-CD-A plays double roles, that is, simultaneously as a cross-linking agent and a carrier to introduce *β*-cyclodextrin structures into the chiral microspheres. We investigated the adsorption capacities of the chiral microspheres toward organic chiral compounds dispersed or dissolved in water. Excitingly, the microspheres showed the anticipated adsorption abilities toward the targets under investigation. Meanwhile, the microspheres also showed noticeable adsorption toward usual organic solvents (with CCl_4, CH_2Cl_2, $CHCl_3$, and toluene as examples) and dye (methyl red as representative). The unique chiral microspheres hopefully find practical applications in wastewater treatment.

2. EXPERIMENTAL SECTION

2.1. Materials. Monomer **1** (**M1**, *S*), monomer **2** (**M2**), and rhodium catalyst, (nbd)$Rh^+B^-(C_6H_5)_4$ (nbd, 2,5-norbornadiene) were prepared by the method reported in previous reports.[38−40] *β*-Cyclodextrin derivative (*β*-CD-A), as structurally presented in Figure 1, was synthesized according to the earlier report.[41] Azobis(isobutyronitrile) (AIBN) was obtained from Beijing Chemical Reagent Company and purified by recrystallization before use. Octadecyl acrylate, poly(vinyl alcohol) (PVA), methyl red, D- and L-proline, and (*R*)-(+)- and (*S*)-(−)-1-phenylethylamine (PEA) were purchased from Aldrich and used as received. Butyl acrylate was bought from Aldrich and distilled under reduced pressure before use. All the other solvents were obtained from Beijing Modern Eastern Fine Chemical Company and distilled under reduced pressure under argon atmosphere. Deionized water was used in all experiments.

2.2. Measurements. Fourier transform infrared (FTIR) spectra were recorded with a Nicolet NEXUS 670 infrared spectrophotometer (KBr tablet). Circular dichroism (CD) and UV−vis absorption spectroscopy measurements were conducted on a Jasco 810 spectropolarimeter. Optical rotations were measured on a JASCO P-1020 digital polarimeter with a sodium lamp (λ = 589 nm) as light source at room temperature. The morphology of the microspheres was observed with a Hitachi S-4700 scanning electron microscope (SEM). Pore analysis was carried out on a BK122W sorption analyzer.

2.3. Synthesis of Microspheres. The microspheres were prepared according to a methodology as schematically illustrated in Figure 1. In the first step, coordination copolymerization of **M1** and **M2** was carried out with (nbd)$Rh^+B^-(C_6H_5)_4$ as catalyst. Synthesis and characterizations of the copolymer referred to the earlier report.[39,42] In the second step, the macro-monomer, octadecyl acrylate, butyl acrylate, and *β*-CD-A went through radical copolymerization via suspension polymerization approach. Details are illustrated in Supporting Information (SI).

2.4. Adsorption Experiments. *2.4.1. Chiral Adsorption.* Chiral adsorption of the microspheres was determined as reported by us earlier.[39,43] All the chiral adsorption experiments were performed by immersing a predetermined amount of microspheres in adsorbate solution (or dispersion) at room temperature. We accomplished chiral adsorption experiments in three cases: (1) adsorbing chiral compounds dissolved in organic solvent (oil-soluble system); (2) adsorbing chiral compounds dissolved in water (water-soluble system); and (3) adsorbing chiral compounds dispersed in water (dispersion system; the compounds are water-insoluble). In the case of oil-soluble systems, *R*- and *S*-PEA were used as chiral compounds and chloroform as solvent. In the case of water-soluble systems, D- and L-proline were used as chiral compounds and water as solvent. For dispersion systems, *R*- and *S*-PEA were used as chiral compounds, while water was used as solvent.

With the oil-soluble system as an example, the major experiment procedure is stated as follows. A chloroform solution (50 mL) of (*R*)-(+)- or (*S*)-(−)-1-PEA (c = 1 mg·mL^{-1}) was prepared and its optical rotation (α_1) was measured. Then, a predetermined amount of microspheres (1 g) was encased in a filter paper and immersed in the

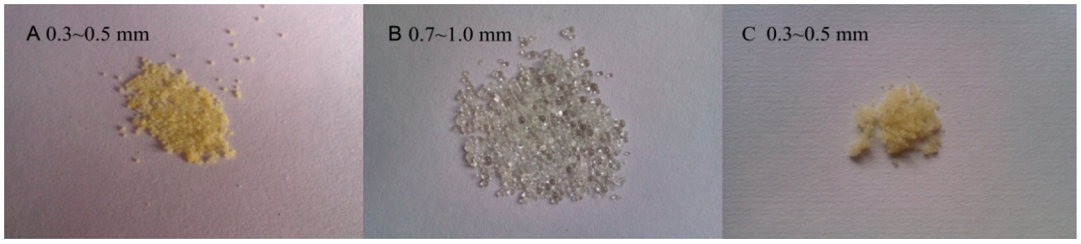

Figure 2. Typical photographs for microspheres: (A) dry microspheres before adsorbing $CHCl_3$, (B) swollen by $CHCl_3$, and (C) after release of $CHCl_3$.

preprepared chiral PEA solution. At regular intervals, the solution was subjected to optical rotation measurement (α_2) with a Jasco digital polarimeter (λ = 589 nm) at room temperature. The chiral compound adsorbed by the microspheres can be calculated according to optical rotations. The chiral absorbency was determined by the following equation: chiral absorbency = $k|(\alpha_2-\alpha_1)/\alpha_1|100$, where k represents the proportional coefficient, determined by working curve approach; α_1 and α_2 are the optical rotations before and after chiral adsorption, respectively. Herein, $|(\alpha_2-\alpha_1)/\alpha_1|$ indicates the absolute values.

To investigate chiral recognition capacity of the microspheres, a term, chiral recognition capacity is defined as the ratio of the difference between the adsorptions by the microspheres toward two enantiomers to the initial weight of the chiral enantiomer in the solution. Since the adsorption is proportional to the corresponding optical rotation, we can determine the chiral recognition capacity of the microspheres by the corresponding optical rotations. Chiral recognition capacity was measured as follows. Taking the oil-soluble system as an example, two enantiomers were mixed in equal amount, forming the so-called racemate. The racemate was dissolved in chloroform (c = 1 mg·mL^{-1}), and the optical rotation of the solution was approximately zero. Then, a predetermined amount of microspheres (1 g) was encased in a filter paper and immersed in the solution. At regular intervals, the solution was subjected to optical rotation measurement (α_3). The chiral recognition capacity can be calculated by the equation: chiral recognition capacity = $(\alpha_3/\alpha_1)100$, where α_1 and α_3 are the optical rotations of the solution (dispersion) before and after adsorption, respectively.

2.4.2. Oil Adsorption. Oil adsorption of the microspheres was separately explored in CCl_4, $CHCl_3$, CH_2Cl_2, and toluene aqueous dispersion (oil/water = 1/10, V/V). The experiment was performed by following our earlier study.[41]

2.4.3. Adsorption of Methyl Red. Adsorption of methyl red was studied by a batch method.[44] Herein, methyl red was taken as a model dye. The detailed operation is shown in SI.

3. RESULTS AND DISCUSSION

3.1. Synthesis of Microspheres. The microspheres were prepared by a two-step method according to the process illustratively presented in Figure 1. First, two *N*-propargylamide monomers (**M1** and **M2**) underwent copolymerization in the presence of Rh catalyst to prepare the helical substituted polyacetylene macro-monomer, in which **M1** was utilized for forming optically active helical polymer chains while **M2** provided the C═C units for the subsequent radical polymerization. Based on the previous investigations, the prepared macro-monomers adopted helical conformations of predominantly one-handed screw sense.[35−39] As the yield of the macro-monomer was nearly 100%, the composition of it was considered keeping nearly consistent with the feed ratio of the monomers.[39] In the second step, the macro-monomer was homogeneously mixed with acrylate monomers (octadecyl acrylate and butyl acrylate) as comonomers and AIBN as initiator. To carry out the free radical suspension polymerization for fabricating the microspheres, β-CD-A was used as the cross-linking agent and PVA as stabilizer. β-CD-A was dissolved in PVA aqueous solution, which was added in the mixture under vigorous stirring until the droplets were uniformly dispersed. When the polymerization system was heated to 60 °C, AIBN decomposed into free radicals to initiate the polymerization in the droplets. As the polymerization proceeded, the droplets transformed into microspheres. Microspheres obtained earlier according to a similar strategy demonstrated enantio-differentiating absorption and release abilities in organic solvent systems.[45] As to be reported below, the microspheres in the present study showed desirable adsorption toward organic compounds in aqueous systems.

The typical photographs of the obtained microspheres are shown in Figure 2. The dried microspheres were rather regular in a spheric morphology (Figure 2A), which maintained well after swelling by $CHCl_3$ (Figure 2B) and even after drying again (Figure 2C). The dried microspheres, 300−500 μm in diameter, showed a pale yellow color (Figure 2A), which originated from the conjugated structures in the helical substituted polyacetylenes, according to our earlier studies.[35−39] After being swollen in chloroform, the microspheres increased to 700−1000 μm and became more transparent and lighter in color (Figure 2B). The swellability of the microspheres is obviously confirmed by the large increase in size. The microspheres returned to the original size and color after the release of chloroform (Figure 2C). The observations also indicate that the microspheres possessed the strength required for the subsequent adsorption experiments.

The microspheres were also observed by scanning electron microscope (SEM), as shown in Figure 3. Figure 3A

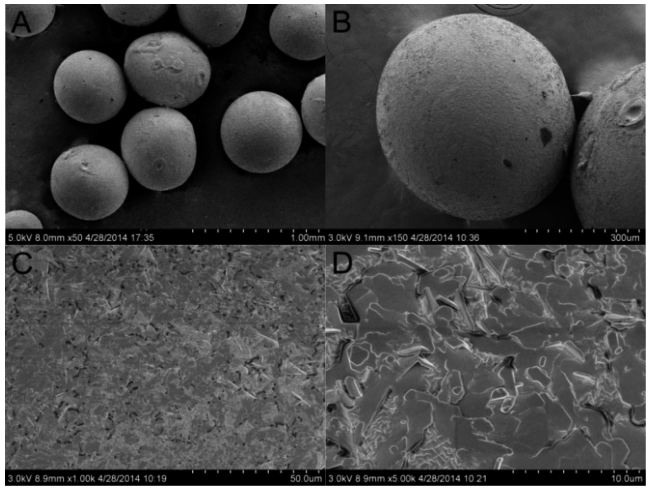

Figure 3. SEM images of the microspheres: (A and B) whole morphology; (C and D) detailed surface structure.

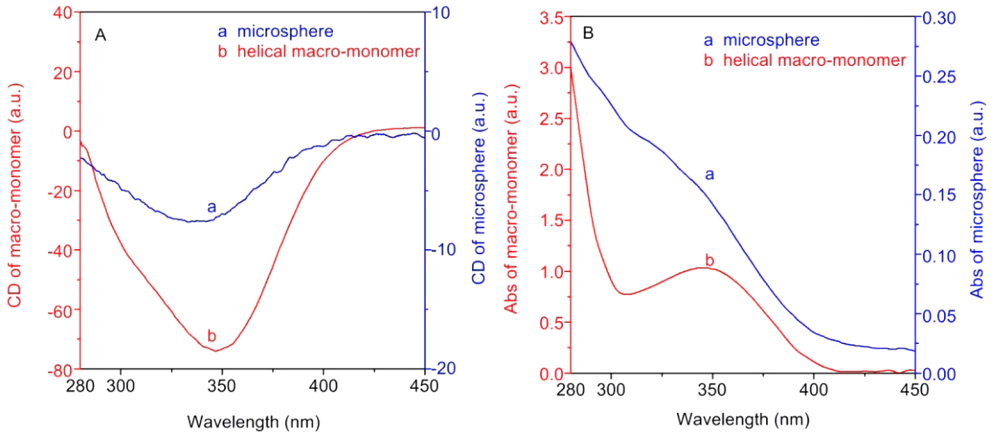

Figure 4. (A) CD spectra of the microspheres and helical macro-monomer; (B) UV−vis spectra of the microspheres and helical macro-monomers. All the spectra were recorded at room temperature.

demonstrates the rather uniform size of the microspheres. The surface of the microspheres is rough and possesses a large number of slit-shaped pores (Figure 3B−D). The large number of pores is desirable in terms of adsorption properties, as to be reported later.

To further analyze the pore structure, nitrogen adsorption/desorption isotherms were measured utilizing the Barrett−Joyner−Halenda (BJH) method to evaluate the pore volume, surface area, and pore size distributions from the adsorption portion of the isotherm to avoid the false peak in desorption portion. The relevant results are presented in Figure S1 (SI). Figure S1A shows that the adsorption and desorption portions in the isotherm are nearly overlapped, leading to an invisible closed hysteresis loop. This type of hysteresis loop indicates the pores in the microspheres are homogeneous and slit-shaped, which is consistent with the observation in SEM images.[46] Figure S1B shows the pore size distribution of the microspheres. The parameters of the pores are BET specific area, 9.322 $m^2 \cdot g^{-1}$; pore volume, 0.112 $cm^3 \cdot g^{-1}$; pore size, 5.541 nm. Just as expected, the BET specific area and pore volume are not large, since we did not add any pore-forming agent in forming the microspheres.

The microspheres were characterized by FTIR spectroscopy. The recorded FTIR spectra are presented in Figure S2 (SI), also including the spectra of helical macro-monomer for a comparison. Detailed analysis on FTIR spectra is also provided therein. Based on the FTIR spectra and referring to our earlier studies,[45] the helical macro-monomer was considered being successfully grafted in the microspheres.

3.2. Optical Activity. The microspheres were characterized by CD and UV−vis spectroscopy, for which the details are provided in SI. According to the previous studies,[39,42] the copolymers derived from **M1** and **M2** showed considerable optical activity resulting from the acetylene-based polymer chains adopting helical conformations of a predominantly one-handed screw sense. Thus, the present microspheres are also expected to possess optical activity. CD and UV−vis spectroscopy have been proved as convincing and efficient means to identify the helical conformations of polyacetylenes[27,32,38] and the optical activity of nano- and microspheres thereof.[26,35−37] Hence, the microspheres were subjected to CD and UV−vis spectroscopy measurements. The obtained spectra are illustrated in Figure 4(A, B).

In Figure 4(A, B), intense CD signals and UV−vis absorption peaks appeared around 350 nm. Referring to our earlier studies,[26,35−37] the CD signal and UV−vis absorption at approximately 350 nm are derived from the helical conformations with predominantly one-handed screw sense formed in substituted polyacetylenes. For a vivid comparison, the spectra of the macro-monomer are also presented in Figure 4. The spectra further demonstrate that helical polyacetylene chains were grafted in the microspheres and endowed the microspheres with optical activity. More interestingly, the helical conformations in the substituted polyacetylenes provide the microspheres with the desired chiral recognition and chiral adsorption abilities, as to be reported below.

3.3. Microspheres without *β*-CD-A. To explore the effects of *β*-CD-A on the microspheres in terms of adsorption, we further prepared microspheres without *β*-CD-A, that is, substituting *β*-CD-A with TMPTA (trimethylolpropane triacrylate) serving as cross-linking agent. Other conditions kept the same as the synthetic procedures for the microspheres in the presence of *β*-CD-A. Figure S3 (SI) shows the photograph of the microspheres without using *β*-CD-A. Briefly, the microspheres with or without *β*-CD-A showed little difference in size and morphology. Also as expected, the microspheres without *β*-CD-A exhibited CD effects and UV−vis absorption around 350 nm (Figure S4 in SI), as observed in the corresponding microspheres with *β*-CD-A (Figure 4). This further demonstrates that the intense CD signal and UV−vis absorption around 350 nm were derived from helical polyacetylene. Adsorption experiments were subsequently conducted with both microspheres with/without *β*-CD-A. Comparing the differences between the microspheres with/without *β*-CD-A in adsorption toward organics, we could elucidate the functions of helical polyacetylene and *β*-CD-A units in the microspheres, as reported below.

3.4. Adsorption Experiments. Our primary purpose of the present study is to prepare microspheres consisting of helical polyacetylene and *β*-CD-A structures and then to explore their potentials as versatile adsorbents toward multiple organic pollutants in wastewater. Therefore, the adsorption experiments were all carried out in water in order to simulate wastewater. The adsorption tests were performed on chiral compounds, organic reagents and organic dye. The microspheres showed encouraging adsorption properties toward these organics under investigation. To achieve deeper insights into the microspheres, the adsorption capacity of the microspheres without *β*-CD-A was also accomplished for a

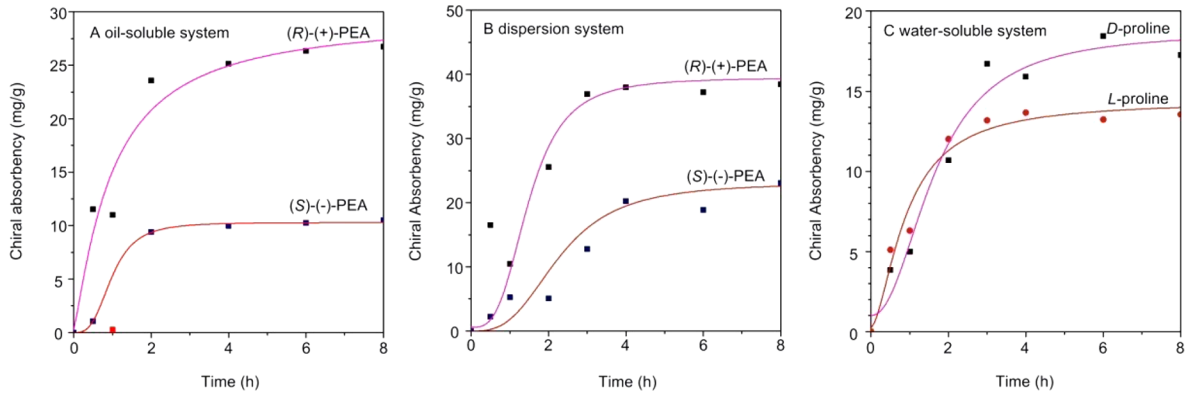

Figure 5. Chiral adsorption of the microspheres with β-CD-A in (A) oil-soluble system in $CHCl_3$, (B) dispersion system in water, (C) water-soluble system (c = 1 mg·mL^{-1}).

comparison to those with β-CD-A. The detailed investigations will be reported below.

3.4.1. Chiral Adsorption of Microspheres. The chiral helical macro-monomer chains in the microspheres theoretically rendered them with chiral adsorption ability. The macro-monomer chains adopted helical conformations of a predominantly one-handed screw sense, which rendered the microspheres with enantioselective adsorption.[47] Enantioselective adsorption results in that one of the enantiomers could preferably enter inside the microspheres. Therefore, the microspheres could preferentially adsorb one enantiomer. We investigated chiral adsorption of the microspheres toward two pairs of enantiomers: D- and L-proline, (*R*)-(+)- and (*S*)-(−)-1-PEA as model chiral adsorbates. The chiral adsorption tests fall into three cases, oil-soluble system, dispersion system, and water-soluble system, as described in detail in Experimental Section. The related results are presented in Figure 5. The microspheres with β-CD-A displayed a remarkably different adsorption toward the enantiomers, predominantly adsorbing (*R*)-(+)-1-PEA and D-proline rather than the corresponding optical isomers. This is true for all the three systems. Taking microspheres in oil-soluble system as example (Figure 5A), the microspheres adsorbed as much as ca. 40% (20 mg·g^{-1}) (*R*)-(+)-PEA after 4 h, while the absorbency was only ca. 17% (8.5 mg·g^{-1}) for (*S*)-(−)-1-PEA. To investigate the saturated absorbency, the microspheres were immersed in the oil-soluble system for 24 h, and the saturated absorbency of (*R*)-(+)-1-PEA was ca. up to 60% (30 mg·g^{-1}), whereas for (*S*)-(−)-1-PEA, it was just 20% (10 mg·g^{-1}). Enantio-differentiating adsorption was also found in the other two systems.

As shown above, the microspheres displayed different adsorptions toward the two enantiomers of interest. This phenomenon is considered resulting from the helical polymer chains forming helices of predominant one-handed screw sense. The helical polymer chains inside the microspheres enantioselectively interacted with (*R*)-(+)-1-PEA and D-proline probably through hydrogen bonds.[48,49] Therefore, the microspheres performed a higher absorbency toward (*R*)-(+)-1-PEA and D-proline than the corresponding enantiomer. In addition, the absorbency of the microspheres in water-soluble system was lower than the other two systems due to their nonswelling in water. So, in this case, adsorbates could not permeate inside the microspheres through swelling process, resulting in the lower absorbency. The microspheres in dispersion system had the highest absorbency. This is because of the extremely low solubility of PEA in water (indeed a heterogeneous system), resulting in high affinity of PEA molecules to the microspheres. Therefore, PEA molecules tended to diffuse inside the microspheres through the voids and channels, during which (*R*)-(+)-1-PEA molecules more easily diffused inside the microspheres due to the enantioselective interactions.[45]

We further explored the chiral recognition capacity of the microspheres in racemate solution in the above three systems. Figure S5A (SI) shows the optical rotation profiles as a function of time, in which the optical rotations were recorded on the residual solution/dispersion. In all the three cases, optical rotation gradually decreased with time prolonging. It demonstrates the microspheres preferentially adsorbed the enantiomers with positive optical rotation, which is consistent with the above observations. Chiral recognition capacity of the microspheres was further determined according to the optical rotations, as described in Experimental Section. Chiral recognition capacity reached the highest in oil-soluble system and the lowest in water-soluble system (Figure S5B). We thus conclude that the chiral recognition capacity of the microspheres was also dependent on the specific adsorbate enantiomers and the specific practice by which to perform the chiral recognition test.

The microspheres with/without β-CD-A are experimentally compared in terms of saturated chiral adsorption, to further elucidate the effects of helical polyacetylene chains and β-CD-A units. The relevant results are illustrated in Figure 6. Herein, the microspheres were immersed in enantiospecific solutions for 24 h to ensure a saturated adsorption. Under identical conditions, the microspheres with β-CD-A showed considerable absorbency of (*R*)-(+)-1-PEA (29 mg·g^{-1}), while for the microspheres without β-CD-A, the adsorption of (*R*)-(+)-1-PEA was only 12 mg·g^{-1} in oil-soluble system. PEA enantiomers showed similar phenomena. Accordingly, a judicious combination of helical polyacetylene and β-CD-A is favorable for achieving chiral adsorption. The unique cyclic structure and large size of cyclodextrin units endowed the microspheres with considerable porous structure.[50] Cavities and channels constructed by cyclodextrin units provide paths for adsorbate molecules to readily pass by. Chiral compounds disperse inside the microspheres through the pores, during which a certain enantiospecific isomer preferentially interacted with the helical polymer chains. As a consequence, this isomer in the two enantiomers is more easily adsorbed by the microspheres.

3.4.2. Oil Absorbency of Microspheres. Apart from chiral compounds, the microspheres under investigation also hope-

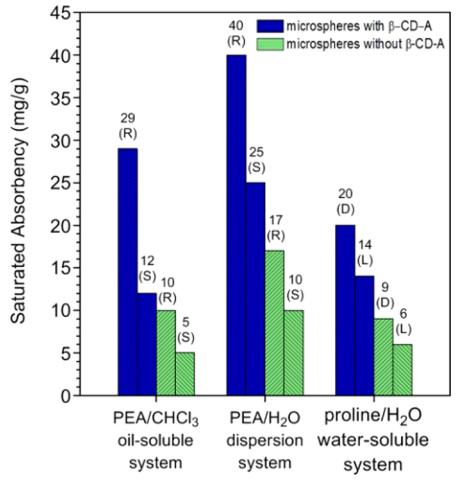

Figure 6. Saturated chiral absorbency of the microspheres with/without β-CD-A in (A) oil-soluble system, (B) dispersion system, and (C) water-soluble system. The number over each bar indicates the corresponding saturated absorbency value.

fully demonstrated high oil-absorbency toward achiral chemicals. In preparing the microspheres, octadecyl acrylate and butyl acrylate, which are expected to provide high swellability, were utilized by referring to our earlier investigations focused on high oil-absorbing resins.[41,45,50] CCl_4, $CHCl_3$, CH_2Cl_2, and toluene were used as model organic compounds to investigate the oil-absorbing ability of the microspheres since the four oils are widely used as industrial solvents and considered being as typical organic contaminants.

Figure 7A illustrates the oil absorbency of the microspheres with β-CD-A in four oils as a function of immersion time. The oil absorbency initially increased with immersion time prolonging, 3 h later reached equilibrium, and remained constant after that. Figure 7B compares the saturated oil absorbency of the microspheres with/without β-CD-A. It shows that β-CD-A noticeably improved the oil absorbency of the microspheres, especially toward CCl_4. This is because β-CD-A provided large cavities and channels[45] for oil molecules to disperse inside the microspheres. The cavities of β-CD-A are nonpolar which can include small molecules with low polarity by inclusion effect. Nonetheless, the adsorption process depends on the adsorbates' solubility parameter, polarity, dimension, diffusion inside the microspheres, etc. These factors made the adsorption a complex process.

3.4.3. Adsorption of Organic Dye. Organic dyes are another category of organic pollutants in wastewater. Herein, methyl red was taken as the organic dye model to conduct the adsorption experiments. The time-absorbency profile of methyl red is presented in Figure 8A. The adsorption rate increased rather rapidly within the first 2 h and then gradually approached adsorption equilibrium. Due to the relatively large specific surface area and the cavities, the microspheres reached the saturated adsorption within approximately 3 h. The maximum absorbency was about 50 $mg \cdot g^{-1}$.

We also compared the saturated absorbency of the two sets of microspheres, that is, with/without β-CD-A units, as displayed in Figure 8B. For the microspheres with β-CD-A, the saturated absorbency of methyl dye was 52 $mg \cdot g^{-1}$, while it was only 17 $mg \cdot g^{-1}$ for the microspheres without β-CD-A. It shows the presence of β-CD-A units largely improved the adsorption ability of the microspheres toward methyl red, due to the cavities and channels constructed by β-CD-A units. This observation is in well agreement with the adsorption of oils and chiral compounds, as discussed above. With good adsorption capacities to multiple adsorbates, the microspheres held large potentials to be used as versatile absorbent toward petroleum derivatives, chiral pharmaceuticals (drugs, pesticides, herbicides, etc.), and organic dyes from wastewater.

3.4.4. Adsorption Mechanism. The time-adsorption profiles toward chiral compounds, oils, and organic dyes (Figure 5, 7, 8) have a common feature. All the curves increased at a rapid speed initially, then flattened out, and finally reached the equilibrium. So, we consider that the adsorptions follow a same mechanism. In order to explore the adsorption mechanism, the pseudo-first-order and the pseudo-second-order models[44,51] were employed to analyze the experimental data by taking the adsorption toward methyl red as example. The pseudo-first-order and the pseudo-second-order kinetic models are respectively represented as

$$\ln(Q_e - Q_t) = \ln Q_e - k_1 t, \qquad \frac{t}{Q_t} = \frac{1}{k_2 Q_e^2} + \frac{t}{Q_e}$$

where k_1 and k_2 are the rate constant for pseudo-first-order (h^{-1}) and pseudo-second-order ($g \cdot mg^{-1} \cdot h^{-1}$) adsorption,

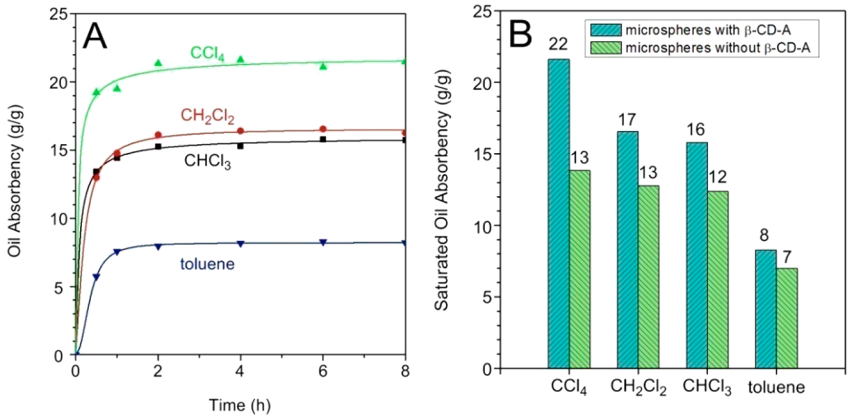

Figure 7. (A) Oil absorbency of the microspheres with β-CD-A toward CCl_4, CH_2Cl_2, $CHCl_3$, and toluene (oil/water = 1/10, V/V). (B) Saturated oil absorbency of the microspheres with/without β-CD-A toward the four organics. The number over each bar indicates the corresponding saturated oil absorbency value.

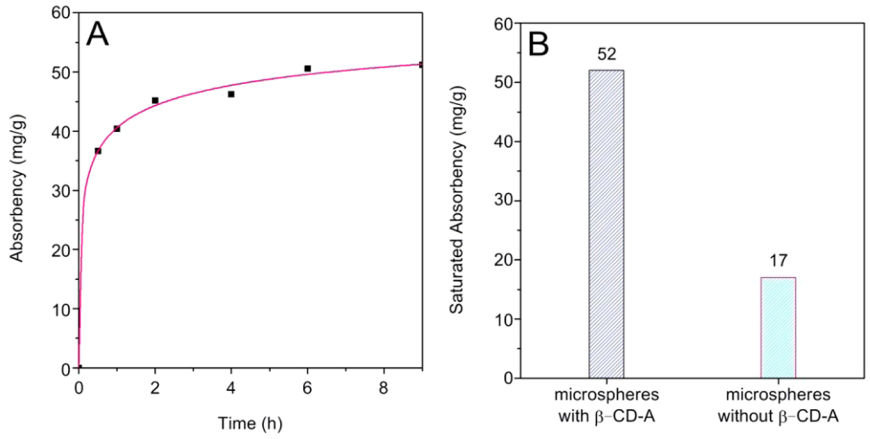

Figure 8. (A) Time-absorbency profile of methyl red on the microspheres (c = 100 mg·L^{-1}). (B) Saturated absorbency of the microspheres with/without β-CD-A toward methyl red.

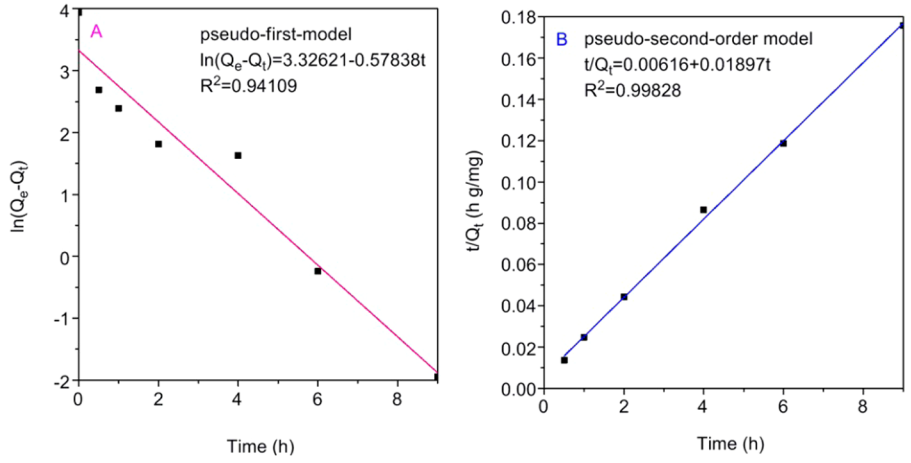

Figure 9. Kinetics models for adsorption of methyl red by the microspheres: (A) pseudo-first-order model; (B) pseudo-second-order model.

Table 1. Parameters of Kinetic Model for Adsorption of Methyl Red on Microspheres

		pseudo-first-order			pseudo-second-order		
initial concn. (mg·L^{-1})	$Q_e{}^a$ (mg·g^{-1})	k_1 (h^{-1})	$Q_e{}^b$ (mg·g^{-1})	R^2	k_2 (g·mg^{-1}·h^{-1})	$Q_e{}^b$ (mg·g^{-1})	R^2
100	51.333	0.578	27.833	0.941	0.0584	52.713	0.998

[a]Calculated by equation in Experimental Section. [b]Calculated by Origin software.

respectively. Q_e and Q_t are the absorbency (mg·g^{-1}) at equilibrium time and time t (h), respectively.

The kinetic curves of the simulation through the computer based on the above two models are shown in Figure 9. The kinetic parameters for adsorption of methyl red by the microspheres are illustrated in Table 1. According to the correlation coefficient (R) of each kinetic model, the pseudo-second-order model was apparently more appropriate for the experimental data. Meanwhile the experimental Q_e value was more accordant with the pseudo-second-order model. Therefore, the adsorption of the microspheres is considered following the pseudo-second-order model rather than the other.

4. CONCLUSIONS

Optically active microspheres were prepared through suspension polymerization by using chirally helical substituted polyacetylene as macro-monomer and β-cyclodextrin-derivative simultaneously as cross-linking agent and porogen agent. The microspheres were obtained in regular morphology and exhibited considerable optical activity and chiral recognition ability. Also, interestingly, the microspheres demonstrated remarkable adsorption capacity toward three sets of organic compounds, including organic chemicals (widely used organic solvents: CCl_4, $CHCl_3$, CH_2Cl_2, and toluene as models), chiral compounds (chiral phenylethylamine and proline enantiomers), and methyl red as representative of organic dyes. With methyl red as representative, the adsorption kinetics model was further discussed. It followed the pseudo-second-order model. With good adsorption capacities to multiple adsorbates, the microspheres held large potentials to be used as versatile absorbent toward petroleum derivatives, chiral pharmaceuticals (drugs, pesticides, herbicides, etc.), and organic dyes from wastewater.

■ ASSOCIATED CONTENT

Supporting Information

Details for synthesis of microspheres; the method for CD and UV−vis spectroscopy measurements; the detailed adsorption

experiment of methyl red; nitrogen adsorption−desorption isotherms and pore size distribution plots; typical FTIR spectra of helical macro-monomer and microspheres; typical photographs for microspheres without β-CD-A; CD and UV−vis spectra of microspheres without β-CD-A; time-optical rotation profiles and time-chiral recognition capacity of the microspheres. This material is available free of charge via the Internet at http://pubs.acs.org.

AUTHOR INFORMATION

Corresponding Author

*Tel: +86-10-6443-5128. Fax: +86-10-6443-5128. E-mail: dengjp@mail.buct.edu.cn.

Notes

The authors declare no competing financial interest.

ACKNOWLEDGMENTS

This work was supported by the National Natural Science Foundation of China (21474007, 21274008, 21174010), the Funds for Creative Research Groups of China (51221002), and the "Specialized Research Fund for the Doctoral Program of Higher Education" (SRFDP 20120010130002).

REFERENCES

(1) Pomiès, M.; Choubert, J.-M.; Wisniewski, C.; Coquery, M. Modelling of Micropollutant Removal in Biological Wastewater Treatments: A review. *Sci. Total Environ.* **2013**, *443*, 733−748.

(2) Guieysse, B.; Norvill, Z. N. Sequential Chemical-Biological Processes for the Treatment of Industrial Wastewater: Review of Recent Progresses and Critical Assessment. *J. Hazard. Mater.* **2014**, *267*, 142−152.

(3) Suo, Z.; Dong, X.; Liu, H. Single-Crystal-Like NiO Colloidal Nanocrystal-Aggregated Microspheres with Mesoporous Structure: Synthesis and Enhanced Electrochemistry, Photocatalysis and Water Treatment Properties. *J. Solid State Chem.* **2013**, *206*, 1−8.

(4) Wang, H.; Yuan, X.; Wu, Y.; Huang, H.; Peng, X.; Zeng, G.; Zhong, H.; Liang, J.; Ren, M. Graphene-Based Materials: Fabrication, Characterization and Application for the Decontamination of Wastewater and Wastegas and Hydrogen Storage/Generation. *Adv. Colloid Interface Sci.* **2013**, *195−196*, 19−40.

(5) Sivakami, M. S.; Gomathi, T.; Venkatesan, J.; Jeong, H.-S.; Kim, S.-K.; Sudha, P. N. Preparation and Characterization of Nano-Chitosan for Treatment Wastewaters. *Int. J. Biol. Macromol.* **2013**, *57*, 204−212.

(6) Paudyal, H.; Pangeni, B.; Inoue, K.; Kawakita, H.; Ohto, K.; Ghimire, K. N.; Alam, S. Preparation of Novel Alginate Based Anion Exchanger from *Ulva japonica* and Its Application for the Removal of Trace Concentrations of Fluoride from Water. *Bioresour. Technol.* **2013**, *148*, 221−227.

(7) Cao, Q.; Liu, Y.; Wang, C.; Cheng, J. Phosphorus-Modified Poly(styrene-co-divinylbenzene)-PAMAM Chelating Resin for the Adsorption of Uranium(VI) in Aqueous. *J. Hazard. Mater.* **2013**, *263*, 311−321.

(8) Schofield, W. C. E.; Bain, C. D.; Badyal, J. P. S. Cyclodextrin-Functionalized Hierarchical Porous Architectures for High-Throughput Capture and Release of Organic Pollutants from Wastewater. *Chem. Mater.* **2012**, *24*, 1645−1653.

(9) Liu, Y. M.; Ju, X. J.; Xin, Y.; Zheng, W. C.; Wang, W.; Wei, J.; Xie, R.; Liu, Z.; Chu, L. Y. A Novel Smart Microsphere with Magnetic Core and Ion-Recognizable Shell for Pb^{2+} Adsorption and Separation. *ACS Appl. Mater. Interfaces* **2014**, *6*, 9530−9542.

(10) Khan, N. A.; Hasan, Z.; Jhung, S. H. Adsorptive Removal of Hazardous Materials Using Metal-Organic Frameworks (MOFs): A Review. *J. Hazard. Mater.* **2013**, *244−245*, 444−456.

(11) Ye, X. L.; Zhang, J.; Chen, H.; Wang, X. H.; Huang, F. Fluorescent Nanomicelles for Selective Detection of Sudan Dye in Pluronic F127 Aqueous Media. *ACS Appl. Mater. Interfaces* **2014**, *6*, 5113−5121.

(12) Qu, X.; Alvarez, P. J. J.; Li, Q. Applications of Nanotechnology in Water and Wastewater Treatment. *Water Res.* **2013**, *47*, 3931−3946.

(13) Dinda, D.; Gupta, A.; Saha, S. K. Removal of Toxi Cr(VI) by UV-Active Functionalized Graphene Oxide for Water Purification. *J. Mater. Chem.* **2013**, *A 1*, 11221−11228.

(14) Zhang, Q.; Wang, N.; Zhao, L. B.; Xu, T. W.; Cheng, Y. Y. Polyamidoamine Dendronized Hollow Fiber Membranes in the Recovery of Heavy Metal Ions. *ACS Appl. Mater. Interfaces* **2013**, *5*, 1907−1912.

(15) Luo, S.; Chai, F.; Wang, T.; Li, L.; Zhang, L.; Wang, C.; Su, Z. Flowerlike g-Fe_2O_3@NiO Hierarchical Core−Shell Nanostructures as Superb Capability and Magnetically Separable Adsorbents for Water Treatment. *RSC Adv.* **2013**, *3*, 12671−12677.

(16) Bui, T. X.; Kang, S.-Y.; Lee, S.-H.; Choi, H. Organically Functionalized Mesoporous SBA-15 as Sorbents for Removal of Selected Pharmaceuticals from Water. *J. Hazard. Mater.* **2011**, *193*, 156−163.

(17) Sunsandee, N.; Ramakul, P.; Pancharoen, U.; Leepipatpiboon, N. Enantioseparation of (*S*)-Amlodipine from Pharmaceutical Industry Wastewater by Stripping Phase Recovery via HFSLM: Polarity of Diluent and Membrane Stability Investigation. *Sep. Purif. Technol.* **2013**, *116*, 405−414.

(18) Kasprzyk-Hordern, B. Pharmacologically Active Compounds in the Environment and Their Chirality. *Chem. Soc. Rev.* **2010**, *39*, 4466−4503.

(19) Kasprzyk-Hordern, B.; Baker, D. R. Enantiomeric Profiling of Chiral Drugs in Wastewater and Receiving Waters. *Environ. Sci. Technol.* **2012**, *46*, 1681−1691.

(20) Huang, Y. M.; Xu, Y.; Li, J.; Xu, W. H.; Zhang, G.; Cheng, Z. N.; Liu, J. W.; Wang, Y.; Tian, C. G. Organochlorine Pesticides in the Atmosphere and Surface Water from the Equatorial Indian Ocean: Enantiomeric Signatures, Sources, and Fate. *Environ. Sci. Technol.* **2013**, *47*, 13395−13403.

(21) Weston, D. P.; Lydy, M. J. Toxicity of the Insecticide Fipronil and Its Degradates Tobenthic Macroinvertebrates of Urban Streams. *Environ. Sci. Technol.* **2014**, *48*, 1290−1297.

(22) Wang, X. Y.; Li, Z.; Zhang, H.; Xu, J. F.; Qi, P. P.; Xu, H.; Wang, Q.; Wang, X. Q. Environmental Behavior of the Chiral Organophosphorus Insecticide Acephate and Its Chiral Metabolite Methamidophos: Enantioselective Transformation and Degradation in Soils. *Environ. Sci. Technol.* **2013**, *47*, 9233−9240.

(23) Smith, D. K. Lost in translation? Chirality Effects in the Self-Assembly of Nanostructured Gel-Phase Materials. *Chem. Soc. Rev.* **2009**, *38*, 684−694.

(24) Bag, D. S.; Alam, S. Chiral Chemical Absorption Property of a Cross-Linked Poly(*N*-isopropyl acrylamide-*co*-sodium acrylate) Thermoresponsive Smart Gel. *Chirality* **2012**, *24*, 506−511.

(25) Kristensen, T. E.; Vestli, K.; Jakobsen, M. G.; Hansen, F. K.; Hansen, T. A General Approach for Preparation of Polymer-Supported Chiral Organocatalysts via Acrylic Copolymerization. *J. Org. Chem.* **2010**, *75*, 1620−1629.

(26) Song, C.; Liu, X.; Liu, D.; Ren, C. L.; Yang, W. T.; Deng, J. P. Optically Active Particles of Chiral Polymers. *Macromol. Rapid Commun.* **2013**, *34*, 1426−1445.

(27) Li, B. S.; Lam, J. W. Y.; Yu, Z.-Q.; Tang, B. Z. Tunable Helical Assemblies of L-Alanine Methyl Ester-Containing Polyphenylacetylene. *Langmuir* **2012**, *28*, 5770−5774.

(28) Ho, R.-M.; Chiang, Y.-W.; Lin, S.-C.; Chen, C.-K. Helical Architectures from Self-Assembly of Chiral Polymers and Block Copolymers. *Prog. Polym. Sci.* **2011**, *36*, 376−453.

(29) Mujahid, A.; Stathopulos, H.; Lieberzeit, P. A.; Dickert, F. L. Solvent Vapour Detection with Cholesteric Liquid Crystals—Optical and Mass-Sensitive Evaluation of the Sensor Mechanism. *Sensors* **2010**, *10*, 4887−4897.

(30) Shundo, A.; Hori, K.; Ikeda, T.; Kimizuka, N.; Tanaka, K. Design of a Dynamic Polymer Interface for Chiral Discrimination. *J. Am. Chem. Soc.* **2013**, *135*, 10282−10285.

(31) Wang, L.; Li, F.; Liu, X.; Wei, G.; Cheng, Y.; Zhu, C. A Helical Chiral Polymer-Based Chromo-Fluorescence and CD Response Sensor for Selective Detection of Trivalent Cations. *J. Polym. Sci., Part A: Polym. Chem.* **2013**, *51*, 4070−4075.
(32) Iida, H.; Tang, Z.; Yashima, E. Synthesis and Bifunctional Asymmetric Organocatalysis of Helical Poly(phenylacetylene)s Bearing Cinchona Alkaloid Pendants via a Sulfonamide Linkage. *J. Polym. Sci., Part A: Polym. Chem.* **2013**, *51*, 2869−2879.
(33) Zhang, C.; Wang, H.; Geng, Q.; Yang, T.; Liu, L.; Sakai, R.; Satoh, T.; Kakuchi, T.; Okamoto, Y. Synthesis of Helical Poly(phenylacetylene)s with Amide Linkage Bearing L-Phenylalanine and L-Phenylglycine Ethyl Ester Pendants and Their Applications as Chiral Stationary Phases for HPLC. *Macromolecules.* **2013**, *46*, 8406−8415.
(34) Medina, D. D.; Goldshtein, J.; Margel, S.; Mastai, Y. Enantioselective Crystallization on Chiral Polymeric Microspheres. *Adv. Funct. Mater.* **2007**, *17*, 944−950.
(35) Chen, B.; Deng, J. P.; Yang, W. T. Hollow Two-Layered Chiral Nanoparticles Consisting of Optically Active Helical Polymer/Silica: Preparation and Application for Enantioselective Crystallization. *Adv. Funct. Mater.* **2011**, *21*, 2345−2350.
(36) Luo, X. F.; Deng, J. P.; Yang, W. T. Helix-Sense-Selective Polymerization of Achiral Substituted Acetylenes in Chiral Micelles. *Angew. Chem., Int. Ed.* **2011**, *50*, 4909−4912.
(37) Zhang, D. Y.; Song, C.; Deng, J. P.; Yang, W. T. Chiral Microspheres Consisting Purely of Optically Active Helical Substituted Polyacetylene: The First Preparation via Precipitation Polymerization and Application in Enantioselective Crystallization. *Macromolecules.* **2012**, *45*, 7329−7338.
(38) Tabei, J.; Nomura, R.; Sanda, F.; Masuda, T. Design of Helical Poly(*N*-propargylamides) that Switch the Helix Sense with Thermal Stimuli. *Macromolecules.* **2004**, *37*, 1175−1179.
(39) Zhou, K.; Tong, L. Y.; Deng, J. P.; Yang, W. T. Hollow Polymeric Microspheres Grafted with Optically Active Helical Polymer Chains: Preparation and Their Chiral Recognition Ability. *J. Mater. Chem.* **2010**, *20*, 781−789.
(40) Schrock, R. R.; Osborn, J. A. π-Bonded Complexes of the Tetraphenylborate Ion with Rhodium(I) and Iridium (I). *Inorg. Chem.* **1970**, *9*, 2339−2343.
(41) Ding, L.; Li, Y.; Jia, D.; Deng, J. P.; Yang, W. T. β-Cyclodextrin-Based Oil-Absorbents: Preparation, High Oil Absorbency, and Reusability. *Carbohydr. Polym.* **2011**, *83*, 1990−1996.
(42) Chen, B.; Song, C.; Luo, X. F.; Deng, J. P.; Yang, W. T. Microspheres Consisting of Optically Active Helical Substituted Polyacetylenes: Preparation via Suspension Polymerization and Their Chiral Recognition/Release Properties. *Macromol. Rapid Commun.* **2011**, *32*, 1986−1992.
(43) Yao, F.; Zhang, D. Y.; Zhang, C. H.; Yang, W. T.; Deng, J. P. Preparation and Application of Abietic Acid-Derived Optically Active Helical Polymers and Their Chiral Hydrogels. *Bioresour. Technol.* **2013**, *129*, 58−64.
(44) Wang, Y.; Qi, Y.; Li, Y.; Wu, J.; Ma, X.; Yu, C.; Ji, L. Preparation and Characterization of a Novel Nano-Absorbent Based on Multi-Cyanoguanidine Modified Magnetic Chitosan and Its Highly Effective Recovery for Hg(II) in Aqueous Phase. *J. Hazard. Mater.* **2013**, *260*, 9−15.
(45) Song, C.; Zhang, C. H.; Wang, F. J.; Yang, W. T.; Deng, J. P. Chiral Polymeric Microspheres Grafted with Optically Active Helical Polymer Chains: A New Class of Materials for Chiral Recognition and Chirally Controlled Release. *Polym. Chem.* **2013**, *4*, 645−652.
(46) Sing, K. S. W.; Everett, D. H.; Haul, R. A. W.; Moscou, L.; Pierotti, R. A.; Rouquerol, J.; Siemieniewska, T. Reporting Physisorption Data for Gas/Solid Systems with Special Reference to the Determination of Surface Area and Porosity. *Pure Appl. Chem.* **1985**, *57*, 603−619.
(47) Li, L.; Du, X. Y.; Deng, J. P.; Yang, W. T. Synthesis of Optically Active Macroporous Poly(*N*-isopropylacrylamide) Hydrogels with Helical Poly(*N*-propargylamide) for Chiral Recognition of Amino Acids. *React. Funct.Polym.* **2011**, *71*, 972−979.
(48) He, J.; Ding, L.; Deng, J. P.; Yang, W. T. Oil-Absorbent Beads Containing *b*-Cyclodextrin Moieties: Preparation via Suspension Polymerization and High Oil Absorbency. *Polym. Adv. Technol.* **2012**, *23*, 810−816.
(49) Scuderi, D.; Le Barbu-Debus, L.; Zehnacker, A. The Role of Weak Hydrogen Bonds in Chiral Recognition. *Phys. Chem. Chem. Phys.* **2011**, *13*, 17916−17929.
(50) Berthod, A. Chiral Recognition Mechanisms. *Anal. Chem.* **2006**, *78*, 2093−2099.
(51) Repo, E.; Warchol, J. K.; Kurniawan, T. A.; Sillanpää, M. E. T. Adsorption of Co(II) and Ni(II) by EDTA-and/or DTPA-Modified Chitosan: Kinetic and Equilibrium Modeling. *Chem. Eng. J.* **2010**, *161*, 73−82.